Live-load distribution of an adjacent box-beam bridge: Influence of bridge deck

Ryan T. Whelchel, Christopher S. Williams, and Robert J. Frosch

- Leaking longitudinal joints are commonly observed in adjacent box-beam bridges and may lead load-rating engineers to assume that there is no load distribution where signs of shear key deterioration are observed.
- This paper discusses a series of load tests that were performed on an existing adjacent box-beam structure with leaking joints to determine the load distribution for a deteriorated adjacent concrete box-beam bridge.
- The study found that deteriorated shear keys are capable of distributing load in an adjacent concrete box-beam bridge, the addition of a concrete deck can restore or improve load distribution for a deteriorated structure where the shear keys have failed, and the load distribution for the rehabilitated structure corresponds well with current design equations.

PCI Journal (ISSN 0887-9672) V. 66, No. 6, November–December 2021.
PCI Journal is published bimonthly by the Precast/Prestressed Concrete Institute, 8770 W. Bryn Mawr Ave., Suite 1150, Chicago, IL 60631.

Leaking longitudinal joints are commonly observed in adjacent box-beam bridges and are often associated with an assumed loss of load distribution at the leaking joint. Evidence of a leaking joint (**Fig. 1**) or the presence of a reflective crack in the deck calls into question the condition of the shear key and the capacity of the shear key to transfer load between beams. The position of shear keys within an adjacent box-beam bridge makes visual inspection impossible, and there is no standard nondestructive inspection method to evaluate the condition of the shear key. In the absence of a dependable inspection, load-rating engineers may assume that there is no load distribution where signs of shear key deterioration are observed.

Investigators have conducted load tests to determine the load distribution of adjacent box-beam bridges exhibiting signs of shear key deterioration.[1,2] Steinburg and colleagues[1] performed load tests on the center span of a three-span adjacent box-beam bridge constructed in 1967 with spans of 47.83 ft (14.58 m), transverse ties at the third points of each span, and a bituminous wearing surface. Center span deterioration consisted of delaminated concrete in the top flange of the exterior beams and minimal efflorescence at the longitudinal joints. Results of the load tests indicated that the distribution factors based on measured strains and deflections were consistent with the distribution factors estimated using equations from the fifth edition of the American Association of State Highway and Transportation Officials' *AASHTO LRFD Bridge Design Specifications*.[3]

Figure 1. Leaking joint of an adjacent box-beam bridge.

Kassner and Balakumaran[2] conducted a series of load tests on one span of an existing adjacent box-beam bridge constructed in 1959 with five spans (consisting of a combination of 40.75 and 41.5 ft [12.42 and 12.65 m] individual spans), a single transverse tie tensioned to 30 kip (133 kN), and a bituminous wearing surface. The bridge deterioration consisted of isolated concrete spalling on two beams due to poor concrete consolidation, as well as efflorescence at longitudinal joints that indicated leaking shear keys. Consistent with the study by Steinburg et al., the results of the load tests revealed that the distribution factors based on measured strains were consistent with the distribution factors estimated using equations from the sixth edition of the AASHTO LRFD specifications,[4] which were unchanged from the fifth edition. These same equations continue to be specified in the 2020 AASHTO LRFD specifications.[5]

Steinburg et al., Kassner and Balakumaran, and Attanayake and Aktan[6] found that a leaking shear key may not indicate loss of load distribution. It should be noted that these studies were conducted on bridges constructed with bituminous wearing surfaces. Load test data are not available for bridges constructed with composite or noncomposite concrete decks that have evidence of leaking shear keys.

For adjacent box-beam bridges with reinforced concrete decks, the deck provides an additional mechanism for load distribution. However, current bridge design specifications do not consider the load distribution offered by this mechanism acting without effective shear keys. Table 4.6.2.2.1-1 of the 2020 AASHTO LRFD specifications provides equations for two load distribution cases for adjacent box-beam bridge systems: cases (f) and (g). Case (f) considers adjacent beams with shear keys and a concrete deck. Case (g) considers adjacent beams with shear keys and transverse post-tensioning to provide compression at the longitudinal joint. When evaluating a Case (f) bridge with shear keys exhibiting signs of deterioration where the integrity of the shear key is in question, the amount of load distribution offered by the concrete deck alone is needed but not specified in the 2020 AASHTO LRFD specifications. Similarly, the *AASHTO Manual for Bridge Evaluation*[7] provides no guidance on the live-load distribution of an adjacent box-beam bridge with a concrete deck and no (or deteriorated) shear keys. Furthermore, there is extremely limited experimental research available regarding the load distribution offered by a concrete deck over adjacent beams without shear keys. The only known research is by Jones,[8] who conducted static load tests on an adjacent box-beam bridge constructed with a 4 in. (100 mm) thick composite concrete deck without shear keys or transverse post-tensioning. Although that study does not present the load distribution for the bridge, the load distribution can be estimated from strains that were measured on the underside of each beam.

Research scope and significance

Considering the general lack of test data and uncertainty in analyzing deteriorated concrete structures, a series of load

tests were conducted to determine the load distribution of a deteriorated adjacent concrete box-beam bridge. Both the load distribution of the existing structure with leaking joints and load distribution after rehabilitation with a noncomposite reinforced concrete deck were investigated. A noncomposite deck (no shear connectors) was selected to provide a cost- and time-effective solution for the rehabilitation of the existing bridge and also to simplify future deck replacements.

The load tests were conducted on a 40 ft (12.2 m) long adjacent precast, prestressed concrete box-beam bridge in Tippecanoe County, Ind. The bridge was tested in four conditions: as built, after removal of the bituminous wearing surface, after the shear keys were disabled, and with a reinforced concrete deck installed. In addition to assessing load distribution of the existing bridge, the results of this study can serve as support for the use of a concrete deck as a rehabilitation strategy to restore load distribution or function as the primary load distribution mechanism of an adjacent box-beam bridge.

Existing bridge

The adjacent box-beam bridge used for this study was constructed in 1957 and designed based on the 1957 edition of the American Association of State Highway Officials' *AASHO Standard Specifications for Highway Bridges*.[9] The single-span bridge consists of seven adjacent precast, prestressed concrete box beams that are 45 in. (1143 mm) wide and 21 in. (533 mm) deep. The total length of the bridge is 40 ft (12.2 m), and the beams span approximately 39 ft (11.9 m) from centerline of bearing to centerline of bearing. Section properties were assumed to be similar to the 1961 Indiana Department of Transportation (INDOT) standard box beam, section B-21-3-9 (**Fig. 2**). Only a portion of the original design drawings is available, and there are no standard drawings from before 1961. The original drawings specified $^{3}/_{8}$ in. (9.5 mm) diameter seven-wire stress-relieved strand with a minimum tensile strength of 250 ksi (1724 MPa). In 1993, the north exterior box beam (beam 7) was replaced with a precast, prestressed concrete box beam of the same overall dimensions (**Fig. 3**). Drawings are also unavailable for this replacement beam.

The number of strands in each beam was determined using ground-penetrating radar (GPR). The 1957 beams were found to have 21 strands, and the 1993 beam had 12 strands. The difference in the number of strands led investigators to conclude that the 1993 replacement beam is reinforced with ½ in. (12.7 mm) diameter strand. The bridge included a bituminous wearing surface, which was estimated to be 5 in. (127 mm) thick based on a GPR survey. The bridge did not include transverse tie rods, and no transverse post-tensioning was provided.

The condition of the existing bridge was investigated prior to testing and is documented in Fig. 3. Investigators found evidence of water leaking through the shear keys between every beam, with the exception of the joint between beams 4 and 5 (Fig. 3). The investigation also revealed deterioration on beams 1 and 7. Minor longitudinal cracking and concrete spalling were observed on the west end of beam 7 (**Fig. 4**), and the investigators assumed that these conditions had a negligible effect on the flexural strength of the beam. Beam 1 had two rust-stained longitudinal cracks approximately 5 ft (1.5 m) long, located at midspan (Fig. 4) and three exposed strands at the east support (Fig. 4).

Testing procedure

The bridge was load tested in four stages, as described in the following sections, to capture the live-load distribution con-

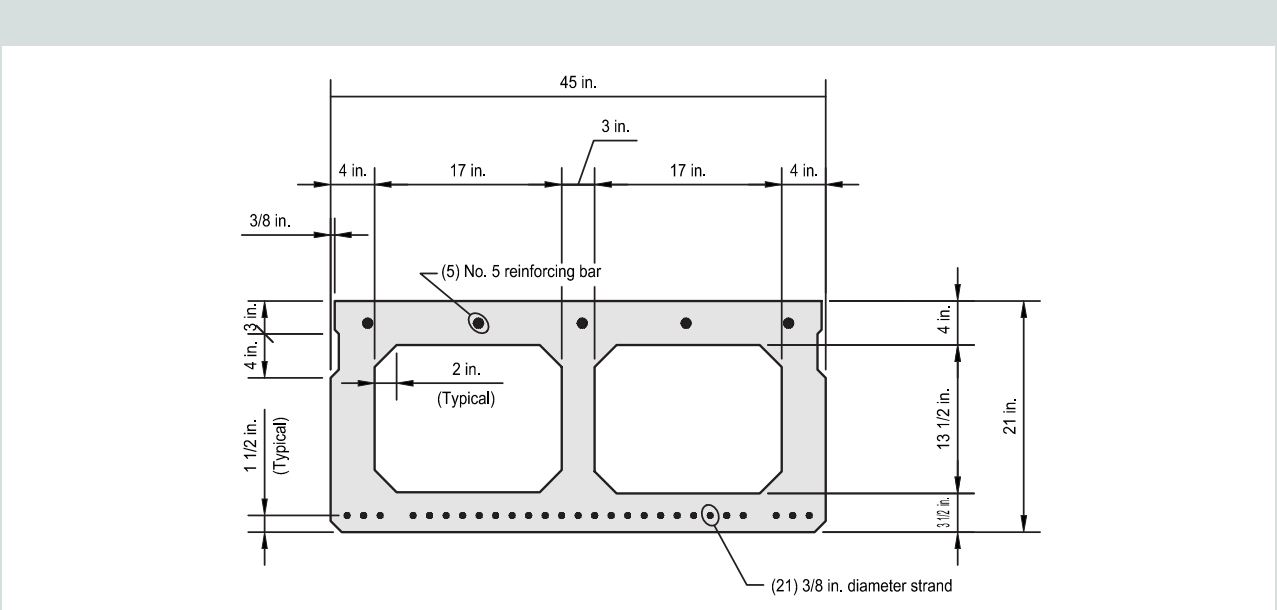

Figure 2. Box-beam cross-section geometry. Note: no. 5 = 16M; 1 in. = 25.4 mm.

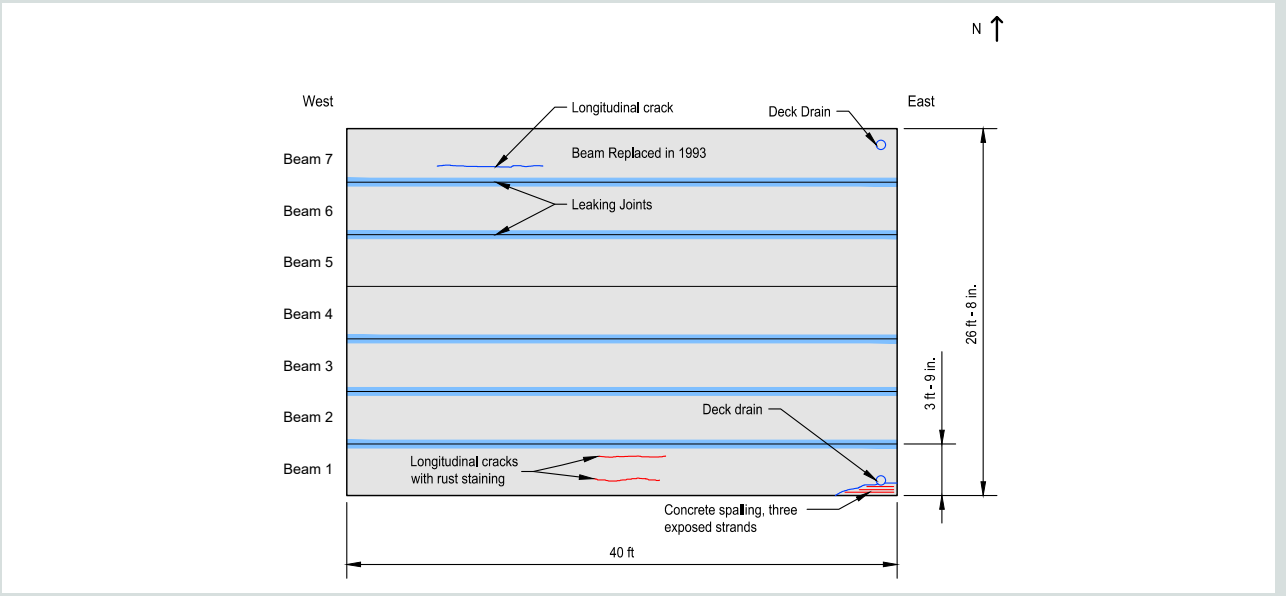

Figure 3. Bottom flange deterioration map of existing bridge. Note: 1 in. = 25.4 mm; 1 ft = 0.305 m.

Longitudinal cracking and minor concrete spalling in west end of beam 7

Rust-stained longitudinal crack on south side of beam 1

Rust-stained longitudinal crack on north side of beam 1

Three exposed strands at east support of beam 1

Figure 4. Bridge deterioration.

sidering four different superstructure conditions. **Figure 5** provides a visual summary of the conditions.

Load test 1: As built

The first load test (LT1) was performed on the bridge as built without any modifications. Beam 1 was not directly loaded because there were concerns regarding the deterioration of the member (Fig. 3).

Load test 2: Wearing surface removed

After LT1 was completed, the bridge was closed to traffic to allow bridge modifications to be completed safely. A bridge contractor removed the bituminous wearing surface. During the milling operation, the milling machine removed a portion of the top flange of each beam and exposed regions of deterioration in beams 1 and 3 that had led to the formation of holes through the flanges (**Fig. 6**). The hole in beam 1 was approximately 10 × 10 in. (254 × 254 mm), and the concrete around the hole had been reduced to rubble over the life of the structure. Both holes in beam 3 were approximately 30 in. (762 mm) long and 10 in. wide after the removal of deteriorated concrete. The holes in each beam were prepared for repair by removing any deteriorated concrete and cleaning the surface around each hole. The contractor then repaired the top flanges by positioning formwork along the bottom of the flange and filling the holes with prepackaged concrete. After the repairs to the top flange of beams 1 and 3 were completed, a second load test (LT2) was performed. As a consequence of the damage to the top flanges, beams 1, 2, and 3 were not directly loaded during the second and third load tests.

Load test 3: Shear keys disabled

A pavement saw, cutting to a depth of 12 in. (305 mm), was used to cut through the entire depth of the shear keys (**Fig. 7**). The third load test (LT3) was performed to verify that the

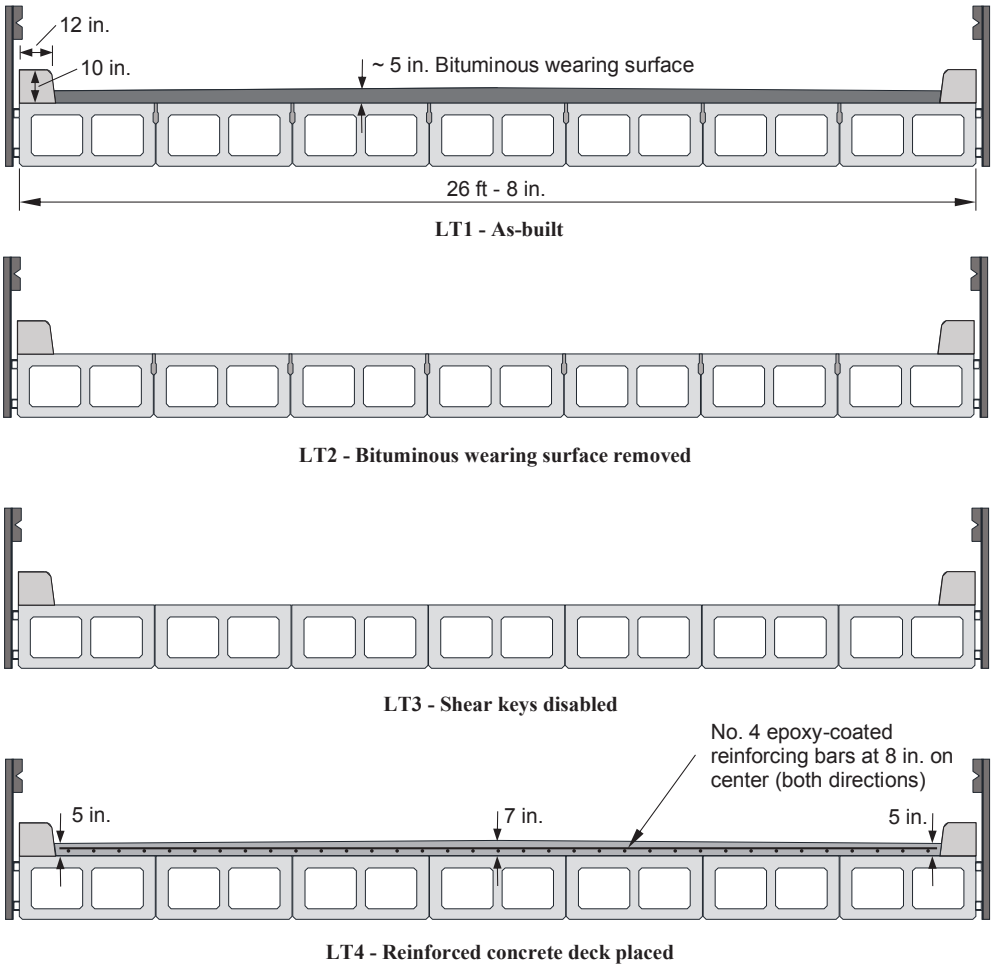

Figure 5. Load test bridge conditions. Note: LT1 = load test 1; LT2 = load test 2; LT3 = load test 3; LT4 = load test 4. No. 4 = 13M; 1 in. = 25.4 mm; 1 ft = 0.305 m.

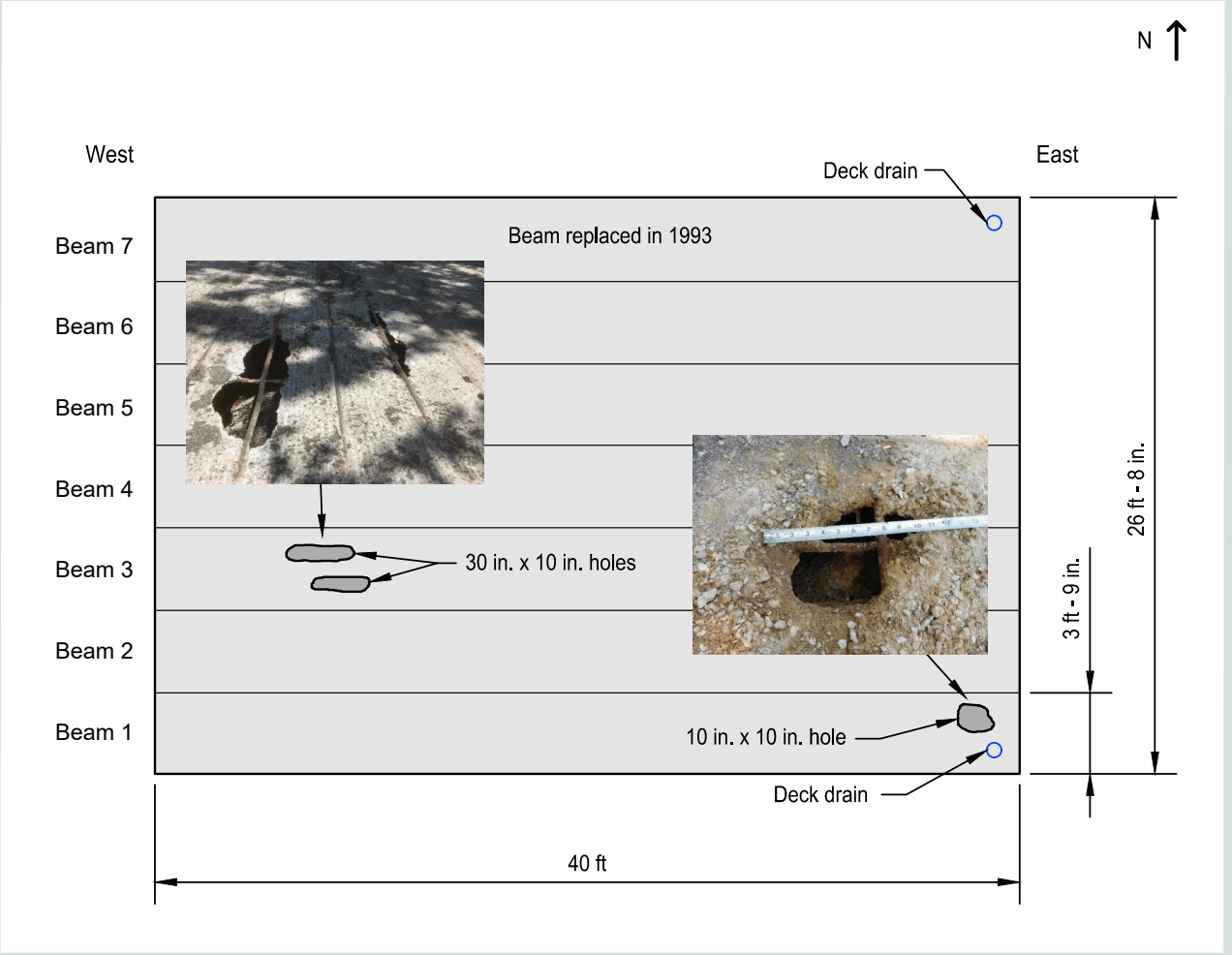

Figure 6. Plan view of the bridge top flange deterioration. Note: 1 in. = 25.4 mm; 1 ft = 0.305 m.

Figure 7. Shear key–cutting operation.

shear keys were disabled and that each beam was acting independently. Disabling the shear keys provides a worst-case scenario for load distribution and allows the contribution of a deck retrofit to load distribution to be fully assessed.

Load test 4: Concrete deck placed

The fourth and final load test (LT4) was performed after a new reinforced concrete deck was placed on the box beams.

Bridge deck

A noncomposite concrete deck was added to the bridge to evaluate its effectiveness in restoring load distribution to a bridge with nonfunctioning shear keys.

Design

The concrete deck was designed using the *Indiana Design Manual*[10] (IDM) and the eighth edition of the 2017 AASHTO LRFD specifications.[11] The deck reinforcement was selected to satisfy the temperature and shrinkage reinforcement requirements of the 2017 AASHTO LRFD specifications. The required area of reinforcement was calculated to be 0.11 in.^{2}/ft (233 mm^2/m). The IDM also specifies an 8 in. (203 mm) maximum spacing for bridge deck reinforcement. This light reinforcement requirement could have been satisfied using no. 3 (10M) reinforcing bars or even welded-wired reinforcement. However, the use of small-diameter reinforcing bars or welded-wire reinforcement in bridge decks is not recommended because workers walking on the reinforcement can easily bend the flexible bars or wires. Bent or displaced reinforcement can lead to difficulties maintaining minimum cover requirements and controlling the effective depth of the reinforcement. Therefore, no. 4 (13M) reinforcing bars at 8 in. maximum spacing were selected (0.3 in.^{2}/ft [635 mm^2/m] area of reinforcement provided) to prevent constructibility issues. To conform with IDM bridge deck reinforcement requirements, Grade 60 (414 MPa) epoxy-coated reinforcing bars were specified.

The IDM specifies that concrete decks must have a minimum top cover thickness of 2.5 in. (63.5 mm) plus 0.5 in. (12.7 mm) for a sacrificial wearing surface. On this project, a minimum bottom cover of 1 in. (25.4 mm) was used to provide for concrete flow under the reinforcement. Using a single mat of no. 4 (13M) reinforcing bars in both directions (1 in. thick), along with the cover requirements, resulted in a total minimum deck thickness of 5 in. (127 mm).

Construction

The surface of each box beam was prepared by sandblasting (**Fig. 8**) to ensure that an adequate bond between the beams and the deck was achieved. The deck was placed in four sections from south to north (Fig. 6), each requiring one concrete truck. The deck thickness was tapered from the bridge centerline to the curb for water drainage. The thickness of the deck was 7 in. (178 mm) at the bridge centerline and 5 in. (127 mm) at each curb line of the transverse section (1.3% cross slope) (Fig. 5). The cross slope was achieved by using tapered formwork at the bridge ends and

Figure 8. Sandblasted box-beam surface.

using a mechanical screed to finish the bridge along the span and across the width (**Fig. 9**). For the final surface finish, the deck was tined after the concrete set. After the surface finish was applied, the deck was covered with wet burlap and plastic for a three-day wet cure.

Materials

The deck concrete mixture proportions (**Table 1**) referenced ASTM standards[12–14] and followed Class C specifications from INDOT's *2018 Standard Specifications*.[15] Concrete cylinders (6 × 12 in. [152 × 305 mm]) were prepared for compression testing from each of the four trucks used for the deck placement. According to Tippecanoe County's construction guidelines, the deck must reach a minimum compressive strength of 4000 psi (27.6 MPa) before a bridge is opened to traffic. All cylinders were cast and stored at the bridge site in accordance with ASTM C31 *Standard Practice for Making and Curing Concrete Test Specimens in the Field*[16] until the cylinders were transported from the site for testing. The graph in **Fig. 10** plots the average concrete compressive strength of the cylinders over time. For each data point, eight cylinders (two from each truck) were tested in accordance with ASTM C39 *Standard Test Method for Compressive Strength of Cylindrical Concrete Specimens*.[17] Figure 10 shows that the concrete met the minimum requirements to be opened to traffic within three days.

Grade 60 (414 MPa) no. 4 (13M) reinforcing bars conforming to ASTM A615 *Standard Specification for Deformed and Plain Carbon-Steel Bars for Concrete Reinforcement*[18] were

Figure 9. Use of mechanical screed and tapered formwork to construct bridge cross slope.

Table 1. Concrete mixture proportions

Material	Type	Quantity
Cement	ASTM C150 Type I	658 lb/ft³
Coarse aggregate	No. 8 limestone (1 in. maximum aggregate size)*	1725 lb/ft³
Fine aggregate	No. 23 natural sand*	1225 lb/ft³
Air entrainment	ASTM C260	3.3 oz/yd³
Water-reducing admixture and retarder	ASTM C494 Type D	19.7 oz/yd³
Water	n/a	249 lb/yd³
Water-cement ratio	n/a	0.38
Specified slump	n/a	4 in.

Note: n/a = not applicable. 1 in. = 25.4 mm; 1 oz/yd³ = 38.681 mL/m³; 1 lb/ft³ = 16.031 kg/m³; 1 lb/yd³ = 0.593 kg/m³.

* Refer to Indiana Department of Transportation (INDOT) standard specifications (INDOT, 2018) for gradation.

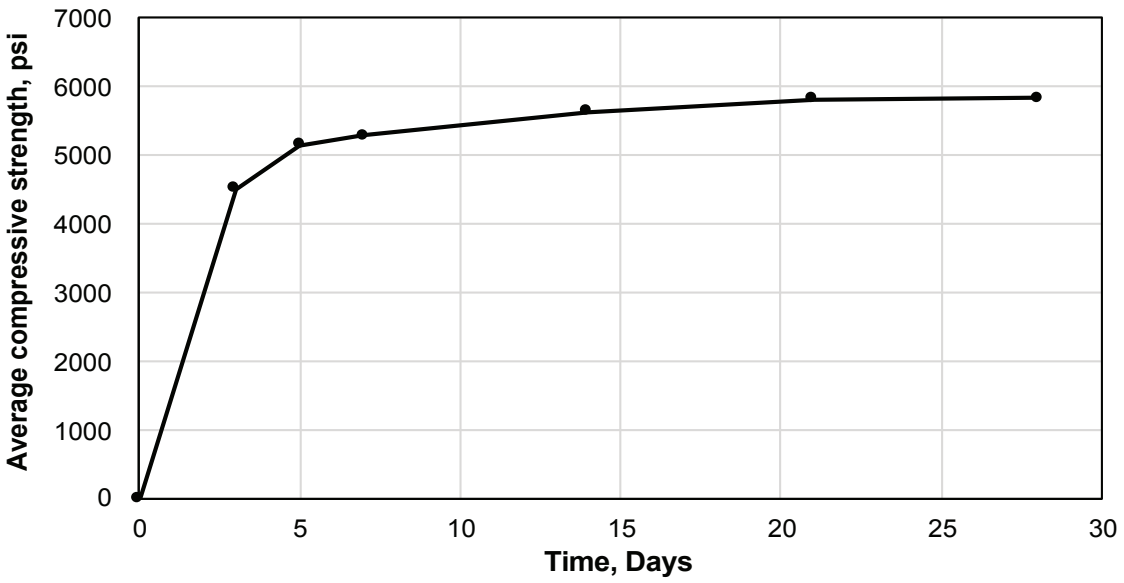

Figure 10. Concrete cylinder compressive strength over time. Note: 1 psi = 6.895 kPa.

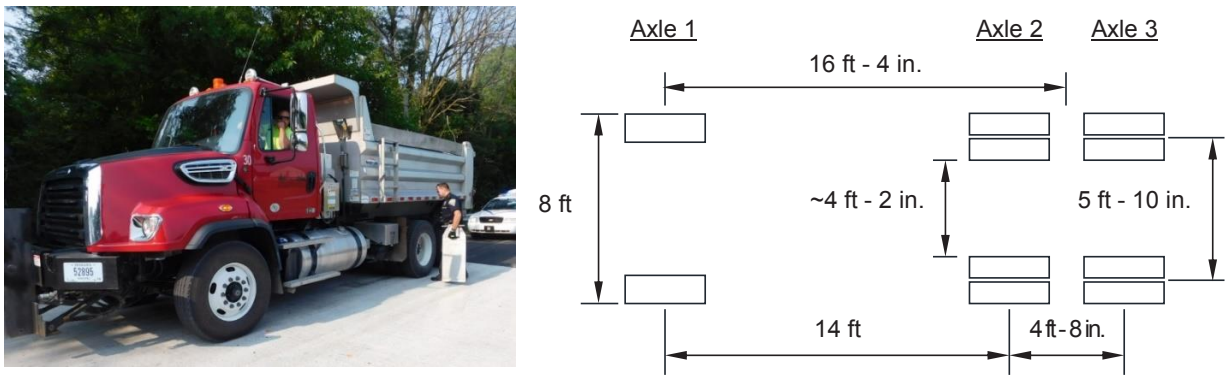

Figure 11. Truck used for load tests and diagram of truck wheel locations. Note: 1 in. = 25.4 mm; 1 ft = 0.305 m.

used for all reinforcement. The measured yield and ultimate tensile strengths of the reinforcing bars were 88 and 104 ksi (607 and 717 MPa), respectively.

Loading procedure

Each of the four load tests was conducted with the same tri-axle truck loaded with gravel. The weight of the vehicle was measured using portable truck-weigh scales from the Indiana State Police Division of Commercial Vehicles. **Figure 11** includes the wheelbase dimensions and axle labels for the truck, and **Table 2** provides the axle weights for each load

Table 2. Truck weights

Load test	Axle 1, lb	Axle 2, lb	Axle 3, lb	Total, lb
LT1	16,450	21,100	20,050	57,600
LT2	15,650	22,300	21,350	59,300
LT3	14,800	15,450	14,450	44,700
LT4	16,450	21,000	21,300	58,750

Note: 1 lb = 4.45 N.

test. A reduced load was used for LT3 because the shear keys were disabled.

A total of 50 load positions—five longitudinal locations along 10 transverse paths—were defined for the bridge. The five positions along the span were selected to approximate the progression of a vehicle crossing the bridge (**Fig. 12**). The 10 transverse paths traveled by the truck were split into five eastbound paths (paths 1 through 5) and five westbound paths (paths 6 through 10). **Figure 13** illustrates the transverse positions of the truck for the 10 paths. The deterioration observed in the site survey and after removal of the bituminous wearing surface prevented some paths from being used for LT1, LT2, and LT3.

Instrumentation

The bridge was instrumented with three linear string potentiometers per beam (21 potentiometers total) to monitor the deflection at the quarter points of each beam. **Figure 14** shows a plan view of the bridge indicating the sensor locations. The potentiometers were mounted on a frame erected on top of scaffolding positioned under the bridge to record absolute deflections. In addition to the potentiometers, concrete strain gauges (90 mm gauge length) were installed on the bottom flange of each beam at midspan as a redundant measurement in the event a potentiometer failed.

Load test results

Figure 15 summarizes the load test results corresponding to position 4 (see Fig. 12 for position location), which is the position where the maximum midspan deflections were recorded. The illustration at the top of Fig. 15 shows the longitudinal position of the truck (position 4) and the direction of travel corresponding to the plots that are provided below the illustration (eastbound for paths 1 through 5 and westbound for paths 6 through 10). A representation of the bridge cross section is illustrated above each deflection plot, and a set of truck tires is shown on top of each cross section to indicate the transverse position of the truck. Midspan deflections of each beam are shown for the truck positioned along all paths. As discussed previously, damage to some beams prevented the loading of some paths. Therefore, paths 4, 5, 9, and 10 were the only paths loaded for all four load tests. A comparison of the results from the eastbound and westbound paths shows the results for both traveling directions were similar.

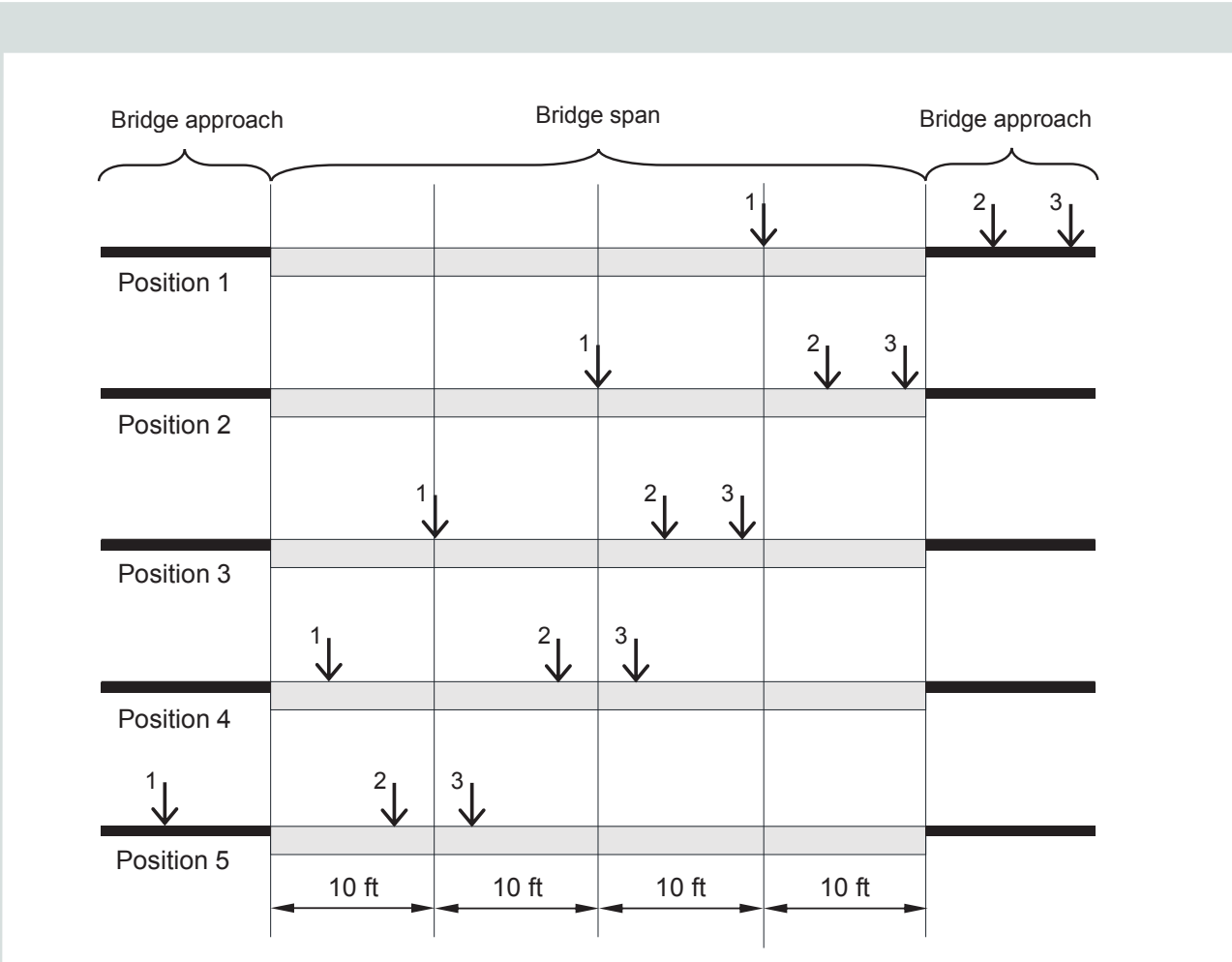

Figure 12. Longitudinal truck positions. Note: Numerical values next to arrows refer to axle labels in Fig. 11. 1 ft = 0.305 m.

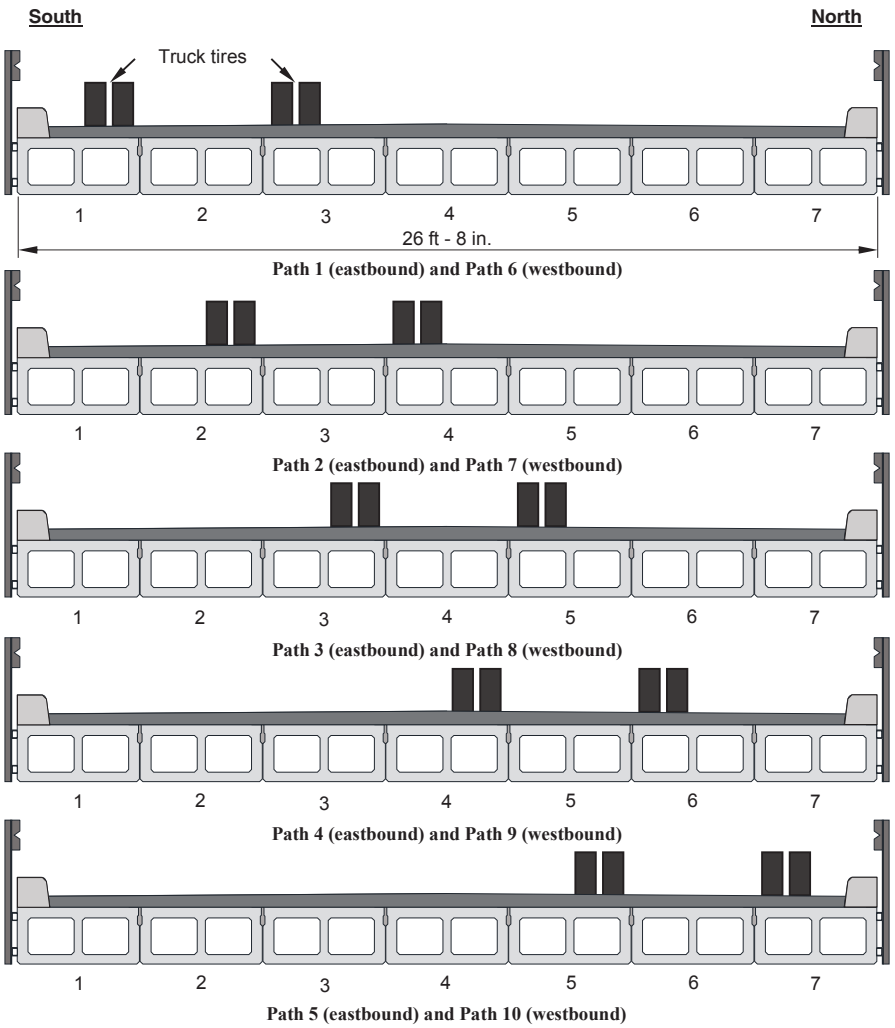

Figure 13. Transverse truck positions during load testing. Note: 1 in. = 25.4 mm; 1 ft = 0.305 m.

LT1: As-built condition

For the first load test, the deflected shape of the transverse section for each path in Fig. 15 shows that a nonzero value of deflection was recorded for every beam. This indicates that every beam was engaged to carry the truck load for each path. Although the longitudinal joints exhibited signs of water leaking through the shear keys, load was distributed to all seven beams for each transverse position. This finding demonstrates that a leaking shear key does not indicate that load transfer has been eliminated or that the shear key is ineffective.

LT2: Wearing surface removed

A comparison of the curves for LT1 and LT2 in Fig. 15 shows that larger deflections were generally measured during LT2 for the beams that were directly loaded. In addition, discontinuities in the transverse deflected shape appear for the beams that were directly loaded.

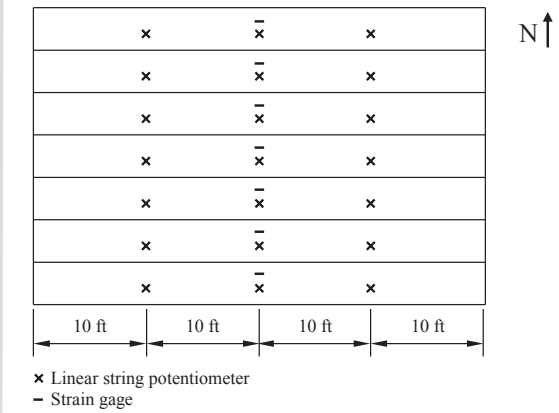

Figure 14. Instrumentation plan. Note: 1 ft = 0.305 m.

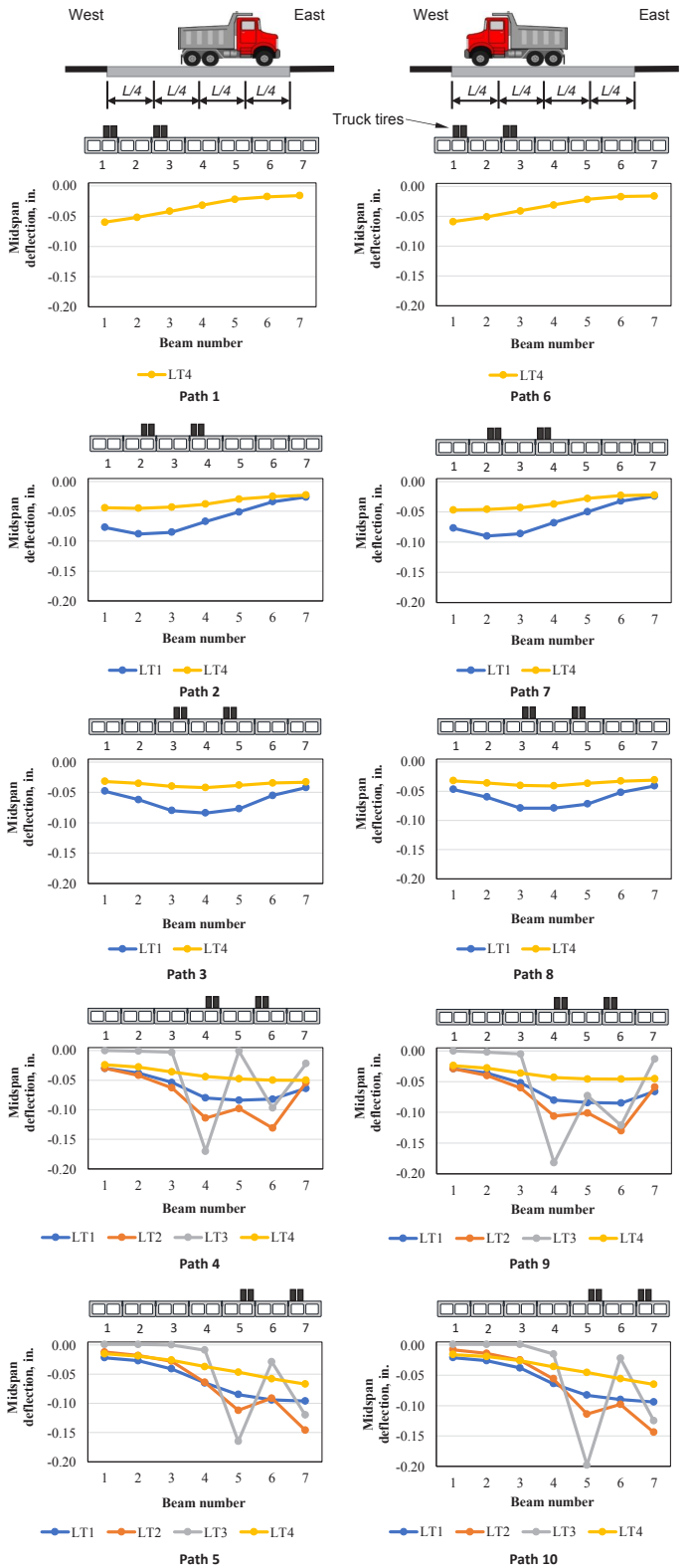

Figure 15. Summary of load test results for truck position 4. Note: The illustration at the top of the figure shows the longitudinal position of the truck (position 4) and the direction of travel corresponding to the plots that are provided below the illustration (eastbound for paths 1 through 5 and westbound for paths 6 through 10). A representation of the bridge cross section is illustrated above each deflection plot, and a set of truck tires is shown on top of each cross section to indicate the transverse position of the truck for the indicated path. *L* = span length; LT1 = load test 1; LT2 = load test 2; LT3 = load test 3; LT4 = load test 4. 1 in. = 25.4 mm.

The increase in measured deflections and the discontinuities in the deflected shape were caused by three factors. First, the milling operation that was conducted between LT1 and LT2 removed a small portion (approximately 0.5 to 2 in. [12.7 to 50.8 mm]) of each beam top flange. The exact reduction in depth could not be accurately measured, but a GPR survey was conducted to estimate the depth to the box-beam void. The depth to the void was then compared to the top flange thickness noted on the 1961 INDOT standard drawing (Fig. 2) to estimate the amount of section lost during the milling operation. Beams 1, 2, and 3 had the greatest loss of top flange thickness (up to approximately 2 in.), whereas beams 4, 5, 6, and 7 were reduced by 0.5 to 1 in. (12.7 to 25.4 mm). The reduction in depth caused a reduction in the moment of inertia, decreasing the flexural stiffness.

Second, removal of the wearing surface and a portion of the top flange (and therefore a portion of the grout between beams) may have allowed slip to occur at the shear keys (**Fig. 16**). The loss of shear key depth increased shear stresses in the keyway, which may have caused the shear key to crack and reduced the shear key's ability to distribute load to adjacent beams. Furthermore, the loss of material reduced the shear stiffness of the shear key.

Finally, removal of the wearing surface itself reduced both the longitudinal flexural stiffness and the transverse joint stiffness. However, considering the relatively low stiffness of the bituminous wearing surface, the contribution of wearing surface removal to the larger deflections of the directly loaded beams is thought to be small relative to the first two factors discussed.

LT3: Shear keys disabled

LT3 was conducted to verify that the shear-key-cutting operation had been successful in disabling the shear keys. Figure 15 shows that the deflected shape for LT3 had large discontinuities at the beams that were directly loaded, indicating the shear keys were disabled. The measured deflections for the beams located between the truck tires were attributable to the proximity of the tires to the shear key joint. The distance between the rear axle tires of the truck was approximately 50 in. (1270 mm), whereas the width of one box beam was 45 in. (1143 mm). Consequently, it was difficult to position the truck so that both rear tires were straddling a beam. However, as shown for paths 4 and 9 in Fig. 15 (in which beams 4 and 6 were directly loaded), no significant loads were transferred to beams 3 and 7. The data for path 4 also show that beam 5 was disengaged. For paths 5 and 10 (in which beams 5 and 7 were directly loaded), beam 4 deflected less than 0.02 in. (0.51 mm), indicating that the beam was effectively disengaged. Although there was some transfer to beam 6 for paths 5 and 10, the large relative deflection between beam 6 and beams 5 and 7 indicates that the key was disengaged but some load was likely applied through the tires. Observation of the lack of load transferred between beams supports the conclusion that the shear keys were disabled.

LT4: Concrete deck added

LT4 was conducted 22 days after the deck was cast. The measured concrete cylinder compressive strength was 5800 psi (40.0 MPa) on the day preceding the load test. Figure 15 compares the results from LT4 and LT1. Although the data from paths 1 and 6 for LT4 cannot be compared to data from LT1, they are presented to provide complete results. The comparison indicates that load distribution was restored by the concrete deck after the shear keys were disabled. A smooth deflected shape is observed for LT1 and LT4. In addition, the deflections measured during LT4 were on average 37% less than the deflections measured during LT1.

The reduction in deflection provides evidence that the concrete deck was acting compositely with the beams even though it was constructed as a noncomposite deck. A simple

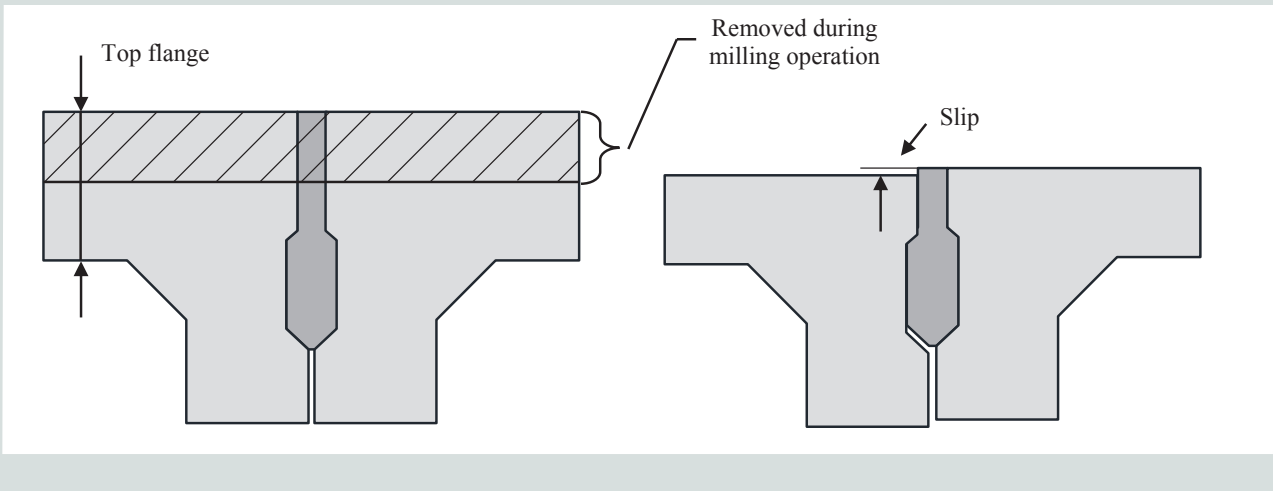

Figure 16. Illustration of shear key slip.

calculation based on the interface shear resistance provisions in Article 5.7.4.3 of the 2020 AASHTO LRFD specifications[5] demonstrated that the cohesion between the concrete deck and concrete box beams for a width of 45 in. (1143 mm) resulted in a factored resistance of 36.5 kip/ft (533 kN/m). The corresponding shear flow generated by the fully factored HL-93 loading on the bridge was calculated to be 28.6 kip/ft (417 kN/m). Therefore, cohesion between the deck and the beams was adequate to transfer the horizontal shear required for composite action under the truck loading.

To further examine the amount of composite action between the box beams and the concrete deck, investigators calculated the estimated midspan deflection of each beam for LT1 $\delta_{est,LT1}$ (no concrete deck) and LT4 $\delta_{est,LT4}$ (considering full composite action) for the truck in position 4 for each load path. When estimating the midspan deflection of each beam, simple support conditions and elastic beam behavior were assumed. The load on each beam was distributed using the midspan deflection data for each load path. Deflections for LT1 were calculated using a moment of inertia of 30,100 in.^{4} (1.25 × 10^{10} mm^4) as calculated for the beam without a concrete deck. Deflections for LT4 were calculated using a moment of inertia of 53,100 in.^{4} (2.21 × 10^{10} mm^4) as calculated for the composite beam and deck. The reduction in midspan deflection between LT1 and LT4 was calculated as $1 - (\delta_{est,LT4}/\delta_{est,LT1})$ for all load cases (**Table 3**). The calculated average reduction in midspan deflection was 39%. The reduction in measured midspan deflection between LT1 and LT4 was calculated as $1 - (\Delta_{LT4}/\Delta_{LT1})$, where Δ_{LT1} and Δ_{LT4} are the measured midspan deflections for LT1 and LT4, respectively. The average reduction in measured midspan deflection was 37% (**Table 4**). This comparison indicates that the concrete deck and concrete box beams exhibited full composite behavior.

Live-load distribution

The proportion of the truck load carried by each beam, herein referred to as live-load distribution, was determined by dividing the midspan deflection of a single beam by the sum of midspan deflections for every beam in the span, as shown in Eq. (1).

$$LLD_i = \frac{\Delta_{mid_i}}{\sum_{i=1}^{7} \Delta_{mid_i}} \quad (1)$$

Table 3. Reduction in estimated deflection calculated as $1 - (\delta_{est,LT4}/\delta_{est,LT1})$

Path	Beam 1	Beam 2	Beam 3	Beam 4	Beam 5	Beam 6	Beam 7
2	0.43	0.49	0.49	0.43	0.42	0.26	0.12
3	0.33	0.44	0.50	0.50	0.50	0.37	0.21
4	0.20	0.26	0.33	0.45	0.43	0.39	0.22
5	0.32	0.30	0.37	0.43	0.45	0.38	0.30
7	0.39	0.49	0.50	0.46	0.44	0.28	0.08
8	0.32	0.40	0.49	0.48	0.49	0.37	0.24
9	0.17	0.22	0.31	0.46	0.46	0.46	0.32
10	0.24	0.27	0.32	0.44	0.45	0.38	0.31

Note: Average reduction = 0.39. $\delta_{est,LT1}$ = estimated midspan deflection for load test 1; $\delta_{est,LT4}$ = estimated midspan deflection for load test 4.

Table 4. Reduction in measured deflection calculated as $1 - (\Delta_{LT4}/\Delta_{LT1})$

Path	Beam 1	Beam 2	Beam 3	Beam 4	Beam 5	Beam 6	Beam 7
2	0.43	0.49	0.49	0.43	0.42	0.25	0.11
3	0.32	0.42	0.49	0.49	0.49	0.36	0.20
4	0.28	0.34	0.40	0.51	0.49	0.45	0.30
5	0.37	0.34	0.41	0.47	0.49	0.43	0.35
7	0.38	0.48	0.50	0.45	0.44	0.28	0.07
8	0.32	0.40	0.49	0.48	0.49	0.37	0.24
9	0.22	0.27	0.35	0.50	0.49	0.49	0.36
10	0.30	0.33	0.37	0.48	0.50	0.43	0.36

Note: Average reduction = 0.37. Δ_{LT1} = measured midspan deflection for load test 1; Δ_{LT4} = measured midspan deflection for load test 4.

where

LLD_i = live-load distribution to beam i (proportion of load carried by beam i)

Δ_{mid_i} = midspan deflection of beam i

i = beam number

By expressing the live-load distribution of each beam in this manner, the results from each load test can be compared independently of both the superstructure's flexural stiffness and variance in the truck's weight.

Wearing surface removed: LT1 compared with LT2

Figure 17 compares the live-load distribution for the load tests LT1, LT2, and LT4. It shows that the live-load distribution of the bridge after the wearing surface was removed (LT2) was reduced compared to the live-load distribution in the original condition (LT1). The live-load distribution was impaired because deflections of the beams that were directly loaded increased relative to the beams that were not directly loaded by the truck. The increase in relative deflection was caused primarily by an increase of slip in the joint (Fig. 16) and a reduction in the stiffness of the shear key, as previously discussed. The contribution of the wearing surface itself to live-load distribution was considered to be minimal.

Concrete deck added: LT1 compared with LT4

By comparing live-load distribution for LT1 and LT4, Fig. 17 shows that the addition of a concrete deck to the bridge without shear keys restored the live-load distribution to a level similar to or greater than that of the bridge in the original condition. For paths 5 and 10 (exterior beams loaded), the live-load distribution was restored to a similar level as the original condition (LT1) by the addition of a concrete deck. For paths 2, 3, 4, 7, 8, and 9 (interior beams loaded), the live-load distribution was improved relative to the original condition.

Table 5. Standard deviation of load distribution

Path	Load test		Difference
	LT1	LT4	
1*	n.d.	0.07	n.d.
2	0.05	0.03	–0.02
3	0.03	0.01	–0.02
4	0.05	0.04	–0.01
5	0.07	0.07	0
6*	n.d.	0.07	n.d.
7	0.06	0.04	–0.02
8	0.03	0.01	–0.02
9	0.05	0.03	–0.02
10	0.07	0.07	0

Note: LT1 = load test 1; LT4 = load test 4; n.d. = no data.

*Deterioration prevented the use of paths 1 and 6 during LT1.

Investigators used the standard deviation of each load distribution curve for all curves loaded in LT1 and LT4 to further compare these two load tests (**Table 5**). The standard deviation provides a metric to describe the difference between the experimental results and a perfect load distribution. A standard deviation of zero indicates that all values in a data set are the same. Therefore, a standard deviation of zero for the load distribution values would indicate that all beams carried equal load. This scenario is considered a perfect load distribution. The population standard deviation was calculated using the load distribution values of beams 1 through 7 for each load path. Comparison of the values in Table 5 indicates that, for all cases, the load distribution provided by the concrete deck was improved or the same as the load distribution of the bridge in its original condition.

Live-load distribution factor

When a simplified beam-line analysis is used to determine the force effects for bridge design, a live-load distribution factor is required to assign a proportion of the force effects to each beam in the bridge.[19] In this investigation, the measured deflection data from the load tests were used to determine the live-load distribution factors for the bridge in its original condition and after the concrete deck had been placed. The distribution factor for the interior beams is defined as the maximum of the live-load distribution values calculated using Eq. (1) for all the interior beams considering all load paths during both LT1 and LT4 (Fig. 17) while the truck was in position 4, the position corresponding with the largest midspan deflections. The distribution factor for the exterior beams is defined similarly and is equal to the maximum live-load distribution (Eq. [1]) of the two exterior beams. **Table 6** provides the maximum distribution factors based on the experimental results.

Although the distribution factors for LT4 are higher than those for LT1, the differences are very small (0.01 and 0.02). Furthermore, the overall behavior of the bridge system improved with the addition of the deck due to the increased flexural stiffness of the bridge, resulting in decreased deflections and reduced stresses in the box beams under service loads.

The distribution factors for LT1 and LT4 are in good agreement with the distribution factors determined by analyzing the strain gauge data from load tests performed by Jones[8] of an adjacent box-beam bridge constructed with a composite concrete deck without shear keys or transverse post-tensioning. For that bridge, the interior and exterior distribution factors were calculated to be 0.26 and 0.23, respectively.

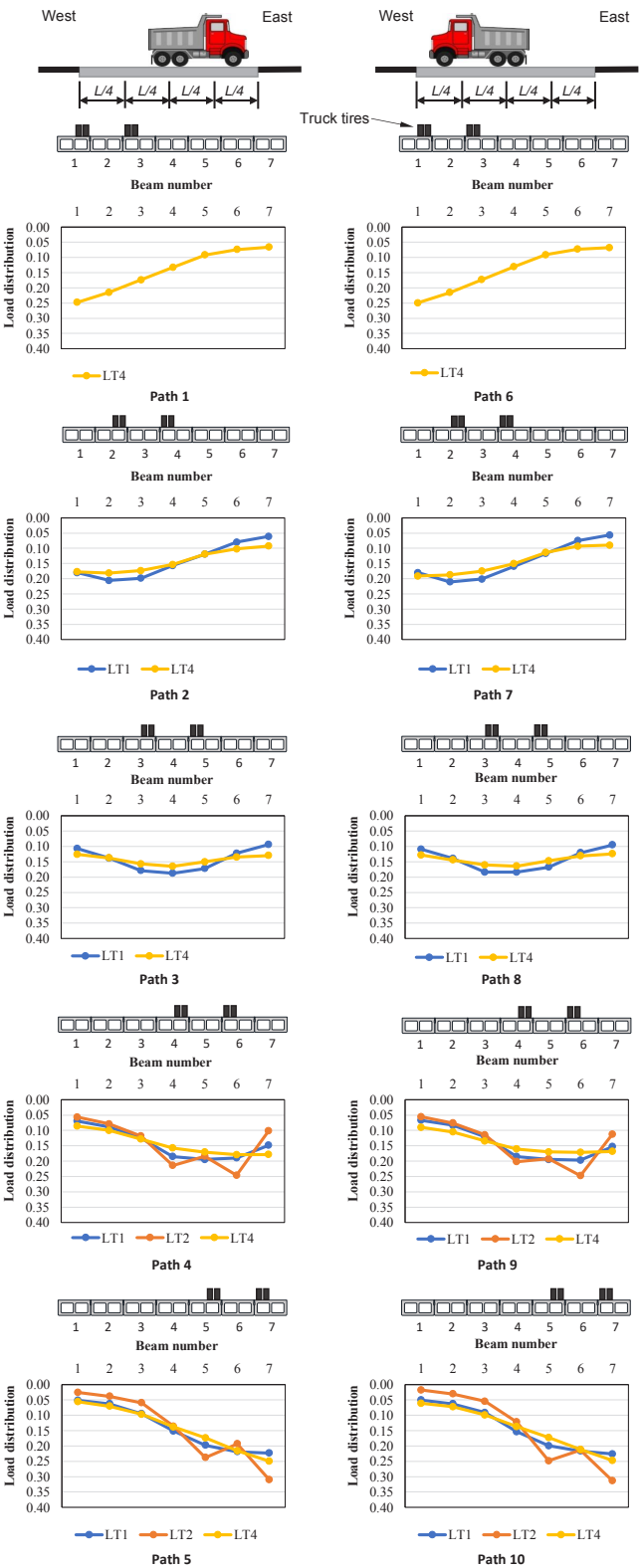

Figure 17. Summary of experimental live-load distribution for truck position 4. Note: The illustration at the top of the figure shows the longitudinal position of the truck (position 4) and the direction of travel corresponding to the plots that are provided below the illustration (eastbound for paths 1 through 5 and westbound for paths 6 through 10). A representation of the bridge cross section is illustrated above each load distribution plot, and a set of truck tires is shown on top of each cross section to indicate the transverse position of the truck for the indicated path. *L* = span length; LT1 = load test 1; LT2 = load test 2; LT3 = load test 3; LT4 = load test 4.

Table 6. Summary of live-load distribution factors

Beam location	Based on load test results		1957 AASHO standard specifications	2002 AASHTO standard specifications	2020 AASHTO LRFD specifications
	As built, LT1	With concrete deck added, LT4			
Interior	0.22	0.23	0.38	0.32	0.21
Exterior	0.23	0.25			0.24

Note: AASHO = American Association of State Highway Officials; AASHTO = American Association of State Highway and Transportation Officials.

1957 AASHO standard specifications live-load distribution factor

The 1957 AASHO standard specifications[9] do not include specific design equations to calculate distribution factors for adjacent beam bridges. The specifications only include guidance for concrete stringers. Assuming that the load distribution expression for concrete stringers was used in the design of the bridge of the current study, the applicable expression from Table 1.3.1 of the AASHO specifications is as follows:

$$load\ fraction = \frac{S}{5.0} \tag{2}$$

where

$load\ fraction$ = wheel-load distribution factor

S = beam spacing

The width of the beam in the bridge is 3.75 ft (1.14 m), resulting in a load fraction value of 0.75. The relationship between the load fraction and the live-load distribution factors in the 2020 AASHTO LRFD specifications[5] is discussed later.

2002 AASHTO standard specifications live-load distribution factor

In article 3.23.4, Eq. (3.11) of the 2002 *AASHTO Standard Specifications for Highway Bridges*,[20] the live-load distribution factor for moment, specified as a wheel-load distribution factor, is expressed as follows:

$$Load\ fraction = \frac{S}{D} \tag{3}$$

where

D = $(5.75 - 0.5N_L) + 0.7N_L(1 - 0.2C)^2$

N_L = number of traffic lanes on the bridge

C = $K(W/L)$ for $W/L < 1$

= K for $W/L \geq 1$

K = $\left[\left(1+\mu\right)\left(\frac{I}{J}\right)\right]^{0.5}$

W = overall width of the bridge

L = span length of the beams

μ = Poisson's ratio of concrete

I = moment of inertia of the beam section

J = torsional constant

The torsional constant J is approximated using Eq. (4):

$$J = \frac{2tt_f\left(b-t\right)^2\left(d-t_f\right)^2}{bt+dt_f-t^2-t_f^2} \tag{4}$$

where

t = web thickness (use single web for multiple web beam)

t_f = flange thickness

b = width of the beam

d = depth of the beam

For the calculation of load distribution, section properties were taken from the 1961 INDOT standard drawing (Fig. 2); Poisson's ratio was assumed to be 0.2, as recommended by the 2002 AASHTO standard specifications; and the number of lanes is 2.[19] The resulting load fraction value calculated from Eq. (3) and Eq. (4) is 0.64.

2020 AASHTO LRFD specifications live-load distribution factors

The 2020 AASHTO LRFD specifications[5] provide an empirical equation for live-load distribution developed by Zokaie et al.[21] To determine the live-load distribution using the 2020 AASHTO LRFD specifications, investigators categorized the bridge in this study as having a Case (f) typical cross section (Table 4.6.2.2.1-1). Then they used the following equation from Table 4.6.2.2.2b-1 of the specifications to estimate the live-load distribution factor for moment in an interior girder $g_{int,m}$:

$$g_{\text{int},m} = k\left(\frac{b}{33.3L}\right)^{0.35}\left(\frac{I}{J}\right)^{0.25} \tag{5}$$

where

k = $2.5(N_b)^{-0.2} \geq 1.5$

N_b = number of beams in the bridge

Similarly, investigators used the following equation from Table 4.6.2.2.2d-1 of the 2020 AASHTO LRFD specifications to calculate the live-load distribution factor for moment in an exterior girder $g_{ext,m}$:

$$g_{ext,m} = g_{\text{int},m}\left(1.125 + \frac{d_e}{30}\right) \quad (6)$$

where

d_e = distance from the centerline of the exterior web to the interior edge of the curb

The curbs of the bridge sit on top of the exterior web of the exterior beam. Therefore, a d_e of 0 ft (0 m) was used for the calculation of $g_{ext,m}$. Using section properties taken from the 1961 INDOT standard drawing (Fig. 2), the live-load distribution factors for moment were calculated from Eq. (5) and (6) to be 0.25 and 0.29 for the interior and exterior beams, respectively.

To compare the live-load distribution factors calculated using the equations in the 2020 AASHTO LRFD specifications to the measured distribution factors, the calculated distribution factors were divided by a multiple presence factor of 1.2 in consideration of the single-lane loading of the load tests. The resulting distribution factors are 0.21 and 0.24 for the interior and exterior beams, respectively.

Discussion

As presented in the preceding sections, the live-load distribution factors in both the 1957 AASHO[9] and 2002 AASHTO standard specifications[20] are given as a "load fraction." These factors are intended to be applied to the wheel load of the standard truck loading, which is equal to half the axle load of the design truck (**Fig. 18**). However, both the live-load distribution factors based on deflection data from the load tests conducted in this study and the live-load distribution factors defined in the 2020 AASHTO LRFD specifications[5] are intended to be applied to the load effect of the entire design truck over the full design lane. Therefore, to compare the distribution factors from both the test data and the 2020 AASHTO LRFD specifications to the load fraction values in the 1957 AASHO and 2002 AASHTO standard specifications, the results of Eq. (2) and (3) must be divided by 2.

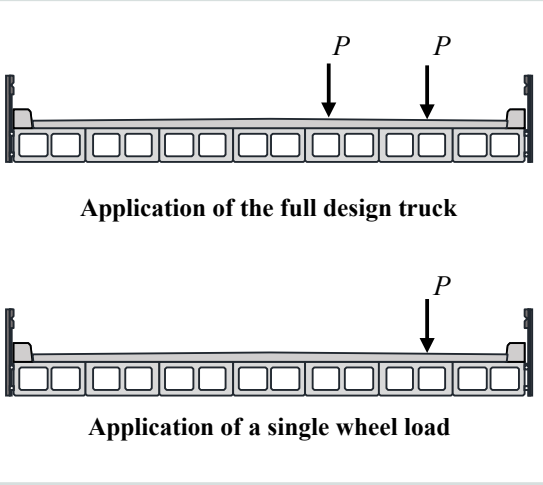

Figure 18. Loading conditions considered for application of live-load distribution factors. Note: *P* = wheel load.

Table 6 summarizes the design live-load distribution factors and the factors based on the load tests. The 1957 and 2002 standard specifications substantially overestimate the distribution factors of the bridge (and resulting demand on the box beams) for both LT1 and LT4. Load ratings performed using the older specifications are therefore conservative. The interior load distribution factor calculated using the expression in the 2020 AASHTO LRFD specifications is in excellent agreement with the experimental results. A similar agreement is observed for the exterior load distribution factors. These results indicate that the live-load distribution factors for moment in the 2020 AASHTO LRFD specifications corresponding to the Case (f) cross section may be used for a bridge with a concrete deck on adjacent box beams without shear keys.

Summary and conclusion

An experimental investigation was conducted on a full-scale adjacent precast, prestressed concrete box-beam bridge in the field. The study included four load tests on the bridge under four conditions: as-built, after removal of the bituminous wearing surface, after the shear keys were disabled, and with a reinforced concrete deck installed. Load was applied using a triaxle truck, and quarter-point deflections of each beam were measured. Load distribution was calculated based on the midspan deflections of each beam when the truck was in the load position corresponding to the maximum recorded deflections. The load distribution was compared among all load tests. Furthermore, the experimental load distribution factors for each load test were determined. The appropriate experimental distribution factors were then compared with the load fraction factors calculated based on the 1957 AASHO[9] and 2002 AASHTO[20] standard specifications, as well as the interior and exterior distribution factors for moment calculated using equations from the 2020 AASHTO LRFD specifications.[5] The primary findings of the investigation are as follows:

- Leaking shear keys are not an indication that load transfer has been eliminated or that the shear keys are ineffective in distributing live load. The test results indicate that even though the shear keys were leaking, live-load distribution was maintained.
- The results of the load tests indicate that the addition of a reinforced concrete deck can restore load distribution even if the primary load distribution mechanism consid-

ered in design (shear keys) is disabled. The addition of a reinforced concrete deck provides an excellent method for improving both the load rating of a deteriorated box-beam bridge and the overall behavior of the bridge.

- A concrete deck placed on concrete beams can achieve full composite action through cohesion between the deck concrete and the concrete beams. The surface should be properly cleaned and roughened prior to placement of the concrete deck. Through composite action, the addition of the deck is not only able to improve load distribution but also can reduce service stresses and deflections of the box beams.

- The load fraction factors calculated based on both the 1957 AASHO and 2002 AASHTO standard specifications were found to be conservative for load rating 1950s-era adjacent box-beam bridges. Similar results are provided by both load fraction equations, and both significantly overestimate the demand on the box beams.

- The expressions in the 2020 AASHTO LRFD specifications for live-load distribution factors for moment provide accurate estimates of the load distribution of an adjacent box-beam bridge. These distribution factors are also appropriate for estimating the live-load distribution factors corresponding to a reinforced concrete deck on adjacent concrete beams without shear keys or with shear keys that are considered damaged or disabled.

Acknowledgments

The authors would like to thank the Indiana Department of Transportation; the Local Technology Assistance Program in Indiana; the Joint Transportation Research Program; and Tippecanoe County, Ind., for making this research possible. The technical perspectives and conclusions reported in this paper are those of the authors, and the authors alone are responsible for the facts and accuracy of the data presented.

References

1. Steinburg, E., R. Miller, D. Nims, and S. Sargand. 2011. *Structural Evaluation of LIC-310-0396 and FAY-35-17-6.82 Box Beams with Advanced Strand Deterioration*. FHWA/OH-2011/16. Columbus, OH: Ohio Department of Transportation, Office of Innovation, Partnerships and Energy. https://www.dot.state.oh.us/Divisions/Planning/SPR/Research/reportsandplans/Reports/2011/Structures/134381_ES.pdf.

2. Kassner, B. L., and S. S. G. Balakumaran. 2017. "Live-Load Test of a 54-Year Old Prestressed Concrete Voided Slab Bridge." Presentation at PCI Convention and National Bridge Conference, February 28–March 4, 2017, Huntington Convention Center, Cleveland, OH.

3. AASHTO (American Association of State Highway and Transportation Officials). 2010. *AASHTO LRFD Bridge Design Specifications*. 5th ed. Washington, DC: AASHTO.

4. AASHTO. 2012. *AASHTO LRFD Bridge Design Specifications*. 6th ed. Washington, DC: AASHTO.

5. AASHTO. 2020. *AASHTO LRFD Bridge Design Specifications*. 9th ed. Washington, DC: AASHTO.

6. Attanayake, U., and H. Aktan. 2013. "First-Generation ABC System, Evolving Design, and Half a Century of Performance: Michigan Side-by-Side Box-Beam Bridges." *Journal of Performance of Constructed Facilities* 29 (3). https://doi.org/10.1061/(ASCE)CF.1943-5509.0000526.

7. AASHTO. 2019. *Manual for Bridge Evaluation, with 2019 Interims Revisions*. Washington, DC: AASHTO.

8. Jones, H. L. 1999. *Multi-Box Beam Bridges with Composite Deck*. FHWA/TX-OO/1709-1. College Station: Texas A&M University. https://static.tti.tamu.edu/tti.tamu.edu/documents/1709-1.pdf.

9. AASHO (American Association of State Highway Officials). 1957. *Standard Specifications for Highway Bridges*. 7th ed. Washington, DC: AASHO.

10. INDOT (Indiana Department of Transportation). 2013. *Indiana Design Manual—2013*. https://www.in.gov/indot/design_manual/design_manual_2013.htm.

11. AASHTO. 2017. *AASHTO LRFD Bridge Design Specifications*. 8th ed. Washington, DC: AASHTO.

12. ASTM International. 2018. *Standard Specification for Portland Cement*. ASTM C150/C150M. West Conshohocken, PA: ASTM International.

13. ASTM International. 2016. *Standard Specification for Air-Entraining Admixtures for Concrete*. ASTM C260/C260M. West Conshohocken, PA: ASTM International.

14. ASTM International. 2017. *Standard Specification for Chemical Admixtures for Concrete*. ASTM C494/C494M. West Conshohocken, PA: ASTM International.

15. INDOT. 2018. *2018 Standard Specifications*. https://www.in.gov/dot/div/contracts/standards/book/sep17/sep.htm.

16. ASTM International. 2018. *Standard Practice for Making and Curing Concrete Test Specimens in the Field*. ASTM C31/C31M. West Conshohocken, PA: ASTM International.

17. ASTM International. 2018. *Standard Test Method for Compressive Strength of Cylindrical Concrete Specimens*. ASTM C39/C39M. West Conshohocken, PA: ASTM International.

18. ASTM International. 2018. *Standard Specification for Deformed and Plain Carbon-Steel Bars for Concrete Reinforcement*. ASTM A615/A615M. West Conshohocken, PA: ASTM International.

19. Barker, R. M., and J. A. Puckett. 1997. *Design of Highway Bridges*. New York, NY: John Wiley & Sons.

20. AASHTO. 2002. *Standard Specifications for Highway Bridges*, 17th ed. Washington, DC: AASHTO.

21. Zokaie, T., T. A. Osterkamp, and R. A. Imbsen. 1991. *Distribution of Wheel Loads on Highway Bridges*. National CHRP 12-26 Final Report Volume 1. Washington, DC: Transportation Research Board. http://onlinepubs.trb.org/onlinepubs/nchrp/docs/NCHRP12-26_FR.pdf.

Notation

b = width of the beam

C = empirical constant

d = depth of the beam

d_e = distance from the centerline of the exterior web to the interior edge of the curb

D = empirical constant

$g_{ext,m}$ = exterior beam live-load distribution factor for moment

$g_{int,m}$ = interior beam live-load distribution factor for moment

i = beam number

I = moment of inertia of beam section

J = torsional constant

k = empirical constant

K = empirical constant

L = span length

$LLDi$ = live-load distribution to beam i (proportion of load carried by beam i)

load fraction = wheel-load distribution factor

N_b = number of beams in the bridge cross section

N_L = number of traffic lanes on the bridge

P = wheel load

S = beam spacing

t = web thickness

t_f = flange thickness

W = overall width of the bridge

$\delta_{est,LT1}$ = estimated midspan deflection for load test 1

$\delta_{est,LT4}$ = estimated midspan deflection for load test 4

ΔLT_1 = measured midspan deflection for load test 1

ΔLT_4 = measured midspan deflection for load test 4

Δ_{mid_i} = midspan deflection of beam i

μ = Poisson's ratio of concrete

About the authors

Ryan T. Whelchel, PhD, is a bridge engineer at Beam, Longest, and Neff. His work is focused on the design, inspection, and rehabilitation of all types of bridges. Whelchel holds a bachelor's degree in architectural engineering from Kansas State University in Manhattan, Kans., and a master's degree and PhD in civil engineering from Purdue University in West Lafayette, Ind. His graduate work concerned the study of the deteriorated behavior of prestressed concrete bridge beams and the nondestructive evaluation of reinforced concrete.

Christopher S. Williams, PhD, is an assistant professor of civil engineering at Purdue University. He received his bachelor of science degree from Southern Illinois University Carbondale and his master of science and PhD from the University of Texas at Austin. He is a consulting member of the PCI Committee on Bridges and the Committee on Bridges Precast Post-tensioned Bridges Subcommittee.

Robert J. Frosch, PhD, PE, FACI, FASCE, is a professor of civil engineering and senior associate dean of facilities and operations in the Purdue University College of Engineering. A fellow of the American Concrete Institute (ACI), he is the editor-in-chief of the *ACI Structural Journal* and serves on the ACI 318 Structural Concrete Building Code Committee, for which he chairs ACI 318D, Structural Members. His research, which focuses on the design and behavior of structural concrete, has resulted in changes to the ACI building code and the American Association of State Highway and Transportation Officials' design specifications.

Abstract

Leaking longitudinal joints are commonly observed in adjacent box-beam bridges and are often associated with an assumed loss of load distribution at the leaking joint. To address the lack of test data and general uncertainty in analyzing deteriorated concrete structures, a series of load tests was conducted to determine the load distribution of a deteriorated adjacent concrete box-beam bridge. Load distribution was investigated for the existing structure with leaking joints as well as for the structure following rehabilitation with a noncomposite reinforced concrete deck. The bridge was tested in four conditions: as built, after removal of the bituminous wearing surface, after the shear keys were disabled, and with a reinforced concrete deck installed. Load distribution was assessed for each condition, and the results were compared with design equations. In addition to assessing load distribution of the existing bridge, the results of this study can serve as support for the use of a concrete deck as a rehabilitation strategy to restore load distribution or function as the primary load distribution mechanism of an adjacent box-beam bridge.

https://doi.org/10.15554/pcij66.6-03

Keywords

Adjacent box-beam bridge rehabilitation, concrete deck, deteriorated prestressed concrete, live-load distribution, load rating, load testing.

Review policy

This paper was reviewed in accordance with the Precast/Prestressed Concrete Institute's peer-review process.

Reader comments

Please address any reader comments to *PCI Journal* editor-in-chief Tom Klemens at tklemens@pci.org or Precast/Prestressed Concrete Institute, c/o *PCI Journal*, 8770 W. Bryn Mawr Ave., Suite 1150, Chicago, IL 60631.